

Equivalent electromagnetic and circuit model for HTS current leads

Streszczenie. Nowoczesne przepusty prądowe urządzeń nadprzewodnikowych budowane są z nadprzewodników wysokotemperaturowych. W artykule zaproponowany został model obwodowo-polowy, który posłuży do analizy funkcjonowania przepustów na bazie nadprzewodnika BSCCO. Model bazuje na fizycznych właściwościach i zachowaniu nadprzewodników wysokotemperaturowych. (Obwodowo-polowy model przepustów prądowych wykonanych z nadprzewodników wysokotemperaturowych)

Abstract. Modern current leads for superconducting devices are built of high temperature superconductors. An equivalent electromagnetic and circuit model that describes the behaviour of a HTS superconducting lead was proposed. The model is based on the physical structure and behaviour of HTS superconductors. First purpose of this model was the numerical analysis of the superconducting current lead built of BSCCO.

Słowa kluczowe: nadprzewodniki wysokotemperaturowe, model obwodowo-polowy, analiza FEM.

Keywords: circuit model, FEM analysis, high temperature superconductors.

Introduction

High temperature superconductors operate at various conditions depending on the application solution. HTS parts are cooled with cryocooler or using cryogenic liquid. When designing the HTS current leads it is very important that they have to lead a very high current with minimal heat supply to the target superconducting device. These two conditions are opposed to each other, larger diameter of the current lead causes an increased flow of current as well as greater amount of heat. The energy losses in practical superconductor are very small under suitable working conditions [11]. However during the quench process the amount of energy in HTS parts rapidly increases. The circuit model of HTS superconductor will improve the processes analysis during the transient states.

High temperature superconducting current leads

Current leads are used for energy transfer between superconducting devices and power supplying system. In such cryogenic application, it is necessary to pass electrical current from a power source at room temperature to a particular device at cryogenic temperatures. These current can range from a few milli-Amperes for instrumentation to 10 000 Amperes for high magnetic field superconducting magnets. The design of cryogenic power leads must attempt to minimize the refrigeration/liquefaction system capacity required for stable operation [1-2],[12].

Considering the fact that cryocoolers in low temperatures, near 3 or 4 Kelvins, have very bad efficiency it is very important to restrict additional energy generated by parts of superconducting device.

Most of HTS current leads are prepared as ceramic tubes made of YBCO or BSCCO superconductors (Fig. 1).



Fig.1. HTS current lead

With HTS development current leads gain new compact design and better capabilities. HTS superconducting current leads architecture usually comprises of HTS tube with silver ends (for better connection) and/or shield made of metal or plastic (Fig. 1 and Fig. 2).



Fig.2. Current leads made of BSCCO tubes [5]

Basing on the practical construction of the current leads produced by CAN Superconductors the equivalent model was prepared. Current lead of type CSL-12/160.2 was modelled with respect of its dimensions and physical properties. (Table 1).

Table 1. Parameters of the sample BSCCO leads [5]

| Type | Dimensions | | | | Critical current (A) | |
|--------------|------------------|--------------|----------------------------------|-----------------------------|----------------------|------|
| | Outer dia. mm | Length mm | Cross section mm ² | Silver contact length mm | 77 K | 64 K |
| CSL-12/160.1 | 12 | 160 | 34 | 12 | 150 | 300 |
| CSL-12/160.2 | 12 | 160 | 34 | 12 | 250 | 500 |
| CSL-12/160.3 | 12 | 160 | 34 | 12 | 370 | 740 |

Usually current leads made of HTS superconductors own the mechanical support which is often made of metal or reinforced plastic (Fig. 3).

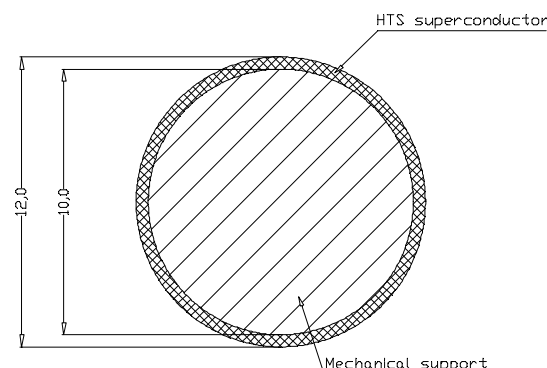


Fig.3. Cross section of the CSL-12/160.2 current lead

The manufacturer supplies additional information on influence of the magnetic field on the critical current and heat leakage of the current lead. The critical current versus magnetic flux is shown in Figure 4.

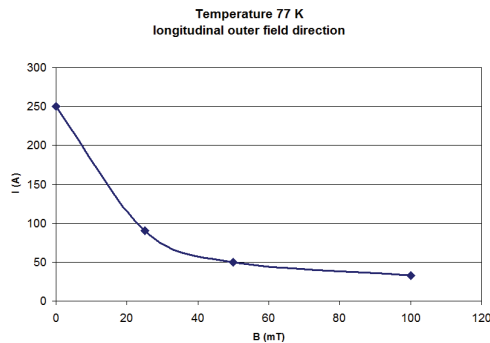


Fig.4. Critical current dependency on the magnetic field in CSL-12/160.2 current lead [3],[5]

The influence of the temperature on the heat leak and the heat leak of the pair of current leads are presented in table 2.

The values of conductive heat leak are given for cooling without vapour; in case of the vapour cooling the values are substantially lower.

Table 2. The conductive heat leak in chosen CSL HTS current leads [5]

| | Conductive heat leak per pair | |
|--------------------|-------------------------------|------------|
| Type | 77 K - 4 K | 64 K - 4 K |
| CSL-12/160.1,.2 | 0.07 W | 0.05 W |
| CSL-12/120.1,.2,.3 | 0.10 W | 0.07 W |
| CSL-18/80.1,.2,.3 | 0.4 W | 0.3 W |

Equivalent electromagnetic and circuit model

The model of HTS current lead was build using FEM package. Geometry of the two dimensional model and generated mesh are shown in Figure 5.

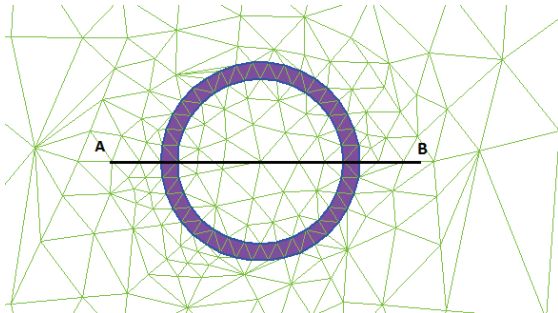


Fig.5. FEM model of the HTS lead with marked analysis AB line

In the model the assumption of no influence of the mechanical support on electromagnetic field was made. Support of HTS current lead is usually made of a material with magnetic permeability close to 1 and high electrical resistivity. Electromagnetic field model was connected with simple electrical circuit. Using the same geometry model the steady state as also as transient state problems can be analysed. Electric circuit consists of voltage source, resistance, HTS current lead and coil as an energy receiver (Fig. 6).



Fig.6. Electrical circuit with HTS lead

The value of the power supply was set to pass current through a HTS lead with value equal to critical current ($I=250$ A in temperature 77K). This provided conditions similar to working critical conditions of current lead. In this study the response of the HTS current lead on critical current in self magnetic field was investigated.

Additionally, in the circuit model the resistances of wires and connections, as well as electromagnet were included.

Moreover, on the base of described above 2D model, the 3D model using FLUX3D software was proposed. The 3D model consists of HTS current lead, the vacuum as the surroundings and a cube reflecting boundary conditions at infinity (Fig. 7). Construction of the 3D model allows you to analyze the physical phenomena in the current lead in the vicinity of other field generated by the devices such as for example superconducting coil or superconducting transformer.

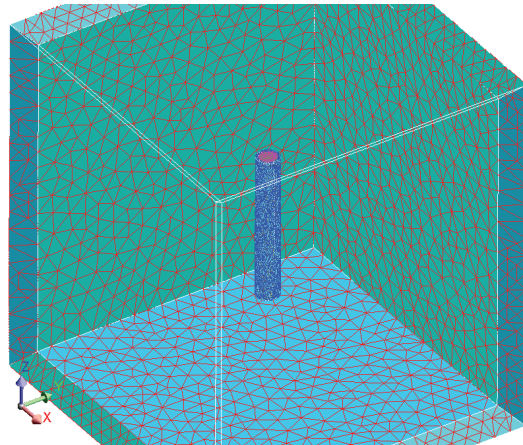


Fig.7. The 3D model of HTS current lead

The properties of modelled HTS current lead was set in this way, that the superconducting state was achieved (lead resistance almost 0 and relative magnetic permeability less than 1). Magnetic properties of BSCCO was modelled in a two different ways. One as constant relative magnetic permeability equal 0.1 and the second with the non-linear B-H curve shown in Figure 8.

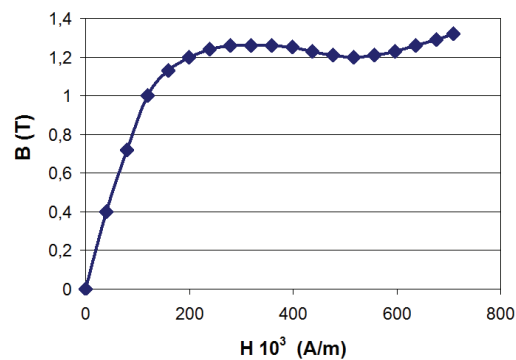


Fig.8. B-H curve of BSCCO superconducting material

The magnetic hysteresis phenomena in HTS superconductors is further discussed in literature and in other works of the author [4],[7-8].

The 3D model was also coupled with circuit model described above.

The 2D problem is formulated as a partial differential equation for the complex amplitude of vector magnetic potential A .

$$(1) \quad \mathbf{B} = \nabla \times \mathbf{A}$$

The flux density \mathbf{B} is assumed to have x and y components, while the vector of electric current density \mathbf{J} and the vector potential \mathbf{A} are orthogonal to it. Only $\mathbf{1}_z \cdot \mathbf{J}_z$ and $\mathbf{1}_z \cdot \mathbf{A}_z$ in planar are not equal to zero. Then simply \mathbf{J} and \mathbf{A} can be denoted. The equation for planar case is

$$(2) \quad \frac{\partial}{\partial x} \left(\frac{1}{\mu_y} \frac{\partial \mathbf{A}}{\partial x} \right) + \frac{\partial}{\partial y} \left(\frac{1}{\mu_x} \frac{\partial \mathbf{A}}{\partial y} \right) - i \omega \sigma \mathbf{A} = -\mathbf{J}_0$$

where: electric conductivity σ and components of magnetic permeability tensor μ_x and μ_y are constants within each block of the model. Source current density \mathbf{J}_0 is assumed to be constant within each model block in planar case.

Total current in a conductor can be considered as a combination of a source current produced by the external voltage and an eddy current induced by the oscillating magnetic field

$$(3) \quad j = j_0 + j_{eddy}$$

Because the field simulation is coupled with electric circuit, the branch equation for a conductor is:

$$(2) \quad I = \frac{U}{R} - i \omega \sigma \int_S A dS$$

where: U is the voltage difference between the two terminals of the solid conductor, and R is the DC resistance of the conductor.

The described formulation ignores displacement current density term in the Ampere's Law. Because the frequency is low and equal 50 Hz the displacement current density is not significant until the operating frequency approaches the MHz values [9],[10].

Results of calculations

The influence of the relative magnetic permeability value of HTS current lead on self magnetic field was investigated. At the Figure 9 the difference in flux density distribution along the AB line for two different relative magnetic permeability models is presented.

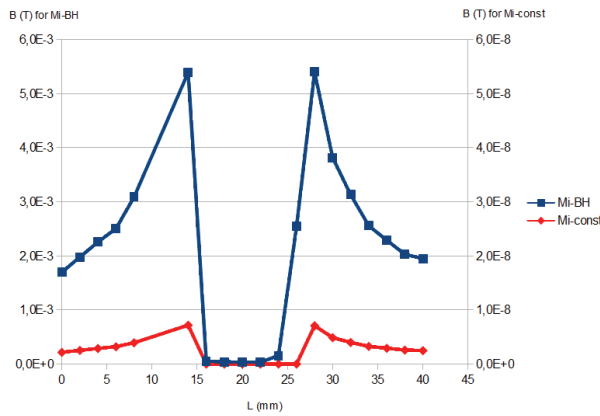


Fig.9. Distribution of the magnetic flux density along the analysis AB line for $\mu=\text{const}$ (red line) and for $\mu=f(H)$ (blue line)

The highest values of magnetic flux density were obtained for nonlinear μ_r given by the BH curve shown in Fig. 9. Comparing the highest value of the self field flux ($B=5.5$ mT) with the dependency of the outer magnetic field on the critical current value (Fig. 4) we can assume that the calculated value is close to that given by the manufacturer.

Therefore for further investigation the nonlinear magnetic permeability model was assumed.

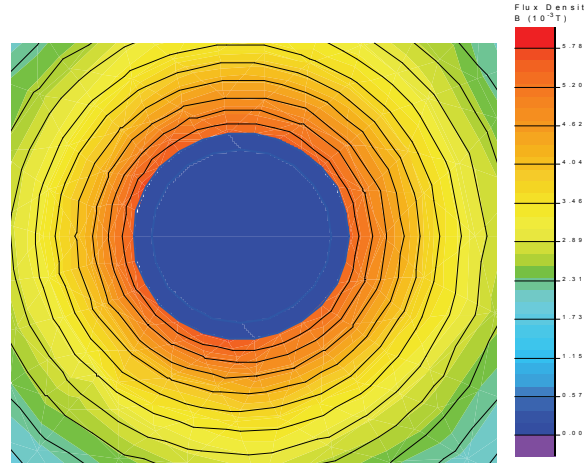


Fig.10. Distribution of the magnetic flux density around the HTS lead

The results of numerical calculations of flux density distribution are shown at Figure 10. The distribution of flux density in the model illustrate that the self magnetic field, derived from lead current flow, does not penetrate the inner parts of HTS current lead.

The voltage and current waveforms in the modelled circuit were observed and shown in Figure 11.

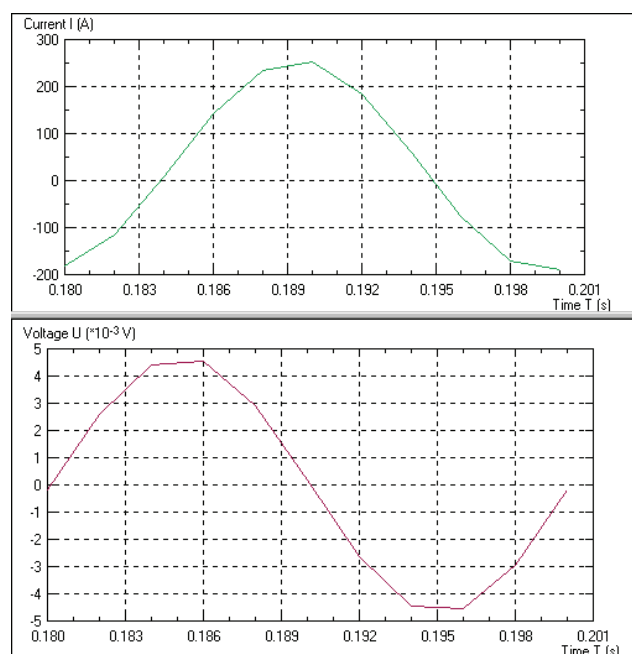


Fig.11. Current and voltage waveforms in HTS current lead

There is a phase shift between the current and voltage because of the inductive receiver and the shapes of waveforms are adequate to the input function. Therefore it can be concluded that developed model allows to observe waveforms of voltage and current in the circuit.

Taking into consideration the relationship between the critical current and magnetic field it can be seen in the Figure 12 that the HTS lead self magnetic field begins play a role at larger currents flowing through a current lead.

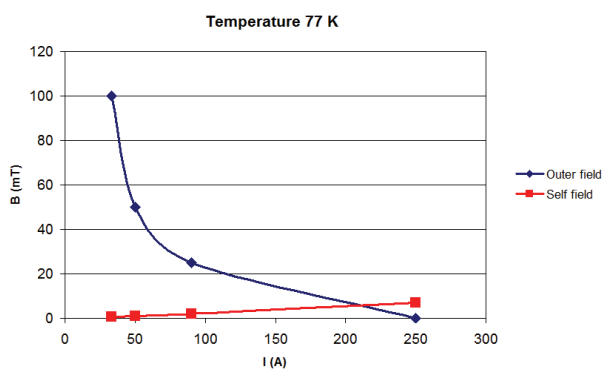


Fig.12. Relations between the self magnetic field versus flowing current and outer magnetic field versus critical current in the HTS lead

The results of calculations in 3D model are presented beneath. The magnetic flux density versus length along transversal symmetry axis is shown in Figure 13.

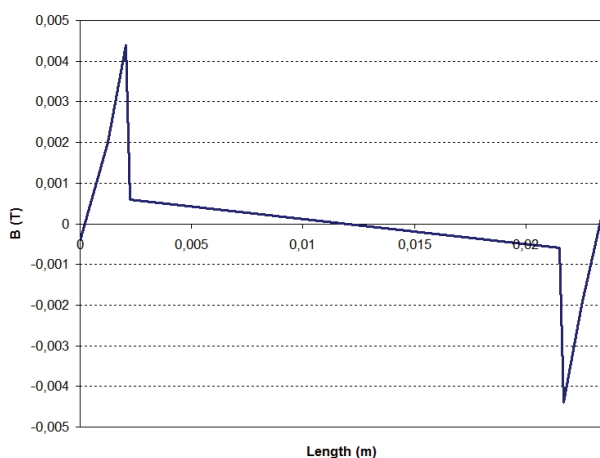


Fig.13. Magnetic flux density versus length along transversal symmetry axis in 3D model of HTS lead

The highest values of magnetic flux can be observed at the surface of HTS current lead.

The distribution of eddy currents in the HTS current lead model has also been designated (Fig. 14).

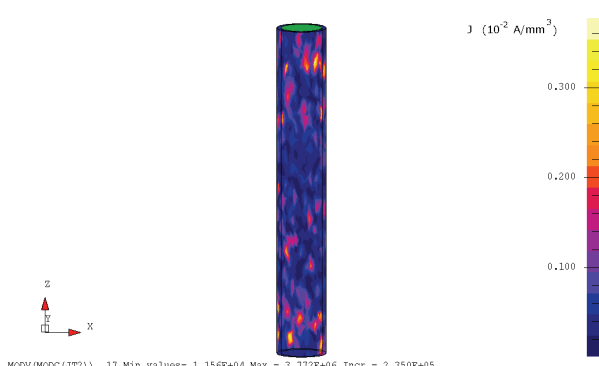


Fig.14. Eddy currents distribution in the 3D model of the HTS current lead

Conclusions

Physical properties of HTS superconductors vary in a wide ranges and their relation to the temperature, current and magnetic field is very difficult for implementation in coupled model representation.

Hysteresis losses are the main part of AC losses in high temperature superconductors.

Combining the electromagnetic model with electrical circuit give better realizability of coupled electromagnetic and electric models. Developed model enable the observation of voltage and current waveforms.

The influence of the magnetic field on the critical current of the HTS current leads is very high.

The proposed model can significantly facilitate the design of HTS current leads.

REFERENCES

- [1] Cyrot M. Pavuna D., Wstęp do nadprzewodnictwa, nadprzewodniki wysokotemperaturowe, PWN rzeszawa 1996.
- [2] Oomen, Marijn Pieter, AC loss in superconducting tapes and cables, Eerste Uitgave 2000, Universiteit Twente
- [3] Kozak S., Janowski T., Kondratowicz-Kucewicz B., Kozak J., Wojtasiewicz G., "Experimental and Numerical Analysis of Energy Losses in Resistive SFCL", IEEE Trans Appl Supercond, 2005, pp. 2098-2101
- [4] Kušević I., Babić E., Marinaro D., Dou S. X., Weinstein R., "Critical currents and vortex pinning in U/n treated Bi2223/Ag tapes", Physica C 408-410 (2004) 524-525
- [5] CAN SUPERCONDUCTORS – High temperature superconductors for practical applications, <http://www.can-superconductors.com/>, 2011
- [6] Janowski, T. Stryczewska, H.D. Kozak, S. Kondratowicz-Kucewicz, B. Wojtasiewicz, G. Kozak, J. Surdacki, P. Malinowski, "Bi-2223 and Bi-2212 tubes for small fault current limiters", IEEE Transactions on Applied Superconductivity, vol. 14, pp. 851 – 854, June 2004
- [7] Czerwiński D., Jaroszyński L., "Analiza numeryczna pola elektromagnetycznych w przepustach prądowych HTS z uwzględnieniem zjawiska histerezy", VIII Seminarium i Warsztaty Zastosowania Nadprzewodników Nałęczów, 2008 r., pp. 122-128
- [8] Jaroszyński L., Czerwiński D., "Modelowanie numeryczne elementów nadprzewodnikowych", VIII Seminarium i Warsztaty Zastosowania Nadprzewodników Nałęczów, 2008, pp. 112-121
- [9] Siahram, M.; Sirois, F., Nguyen, D.N.; Babic, S.; Ashworth, S.P., "Fast Numerical Computation of Current Distribution and AC Losses in Helically Wound Thin Tape Conductors: Single-Layer Coaxial Arrangement", IEEE Transactions on Applied Superconductivity, 2010, Vol. 20 I.6, pp. 2381 - 2389
- [10] Safran, S.; Vojenciak, M., Gencer, A.; Gomory, F., "Critical Current and AC Loss of DI-BSCCO Tape Modified by the Deposition of Ferromagnetic Layer on Edges", IEEE Transactions on Applied Superconductivity, 2010, Vol. 20 I.5, pp. 2294 – 2300
- [11] Majka M., Kozak S., "Zastosowanie taśm I i II generacji do budowy nadprzewodnikowych ograniczników prądu", Przegląd Elektrotechniczny, 2009, nr 5
- [12] Goddard K., Łukasik B., Rotaru M., Sykulski J., "Design study of a high temperature superconducting generator with YBCO windings", Przegląd Elektrotechniczny, 2010, nr 5

Author: dr inż. Dariusz Czerwiński, Politechnika Lubelska, Instytut Podstaw Elektrotechniki i Elektrotechnologii, ul. Nadbystrzycka 38A, 20-618 Lublin, E-mail: d.czerwinski@pollub.pl